Cell Reports
Physical Science

Article

Multi-layer screen-printing of magnetic soft robots with integrated materials and functions

Graphical abstract

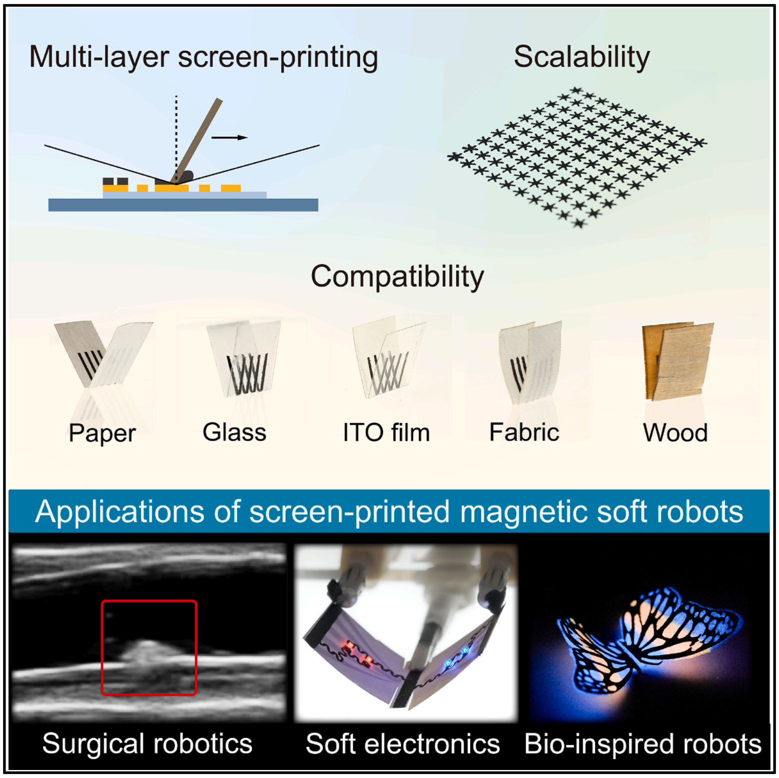

Highlights

- Screen-printing generates multifunctional soft robots comprising various materials
- Magnetic programming enables customized actuation profiles for specific components
- Printing on various substrates broadens the application scenarios of soft robots
- Integrating functional materials and electrical components showcases potential use

Authors

Zhuoyue Wang (王卓越), Sarthak Misra, Venkatasubramanian Kalpathy Venkiteswaran

Correspondence

z.wang01@umcg.nl (Z.W.), v.kalpathyvenkiteswaran@utwente.nl (V.K.V.)

In brief

Magnetic soft robots offer programmable shape-morphing capabilities through magnetic field actuation. To overcome current limitations on manufacturing scalability and material compatibility, Wang et al. introduce a screen-printing strategy for fabricating robots with customized magnetic profiles and materials, enabling the efficient production of multifunctional robots for drug delivery, flexible electronics, and biomimicry.

Wang et al., 2025, Cell Reports Physical Science *6*, 102614
June 18, 2025
https://doi.org/10.1016/j.xcrp.2025.102614

Please cite this article in press as: Wang et al., Multi-layer screen-printing of magnetic soft robots with integrated materials and functions, Cell Reports Physical Science (2025), https://doi.org/10.1016/j.xcrp.2025.102614

Cell Reports
Physical Science

CellPress
OPEN ACCESS

Article

Multi-layer screen-printing of magnetic soft robots with integrated materials and functions

Zhuoyue Wang (王卓越),[1,3,*] Sarthak Misra,[1,2] and Venkatasubramanian Kalpathy Venkiteswaran[2,*]

[1]Department of Biomaterials and Biomedical Technology, University of Groningen and University Medical Centre Groningen, Groningen 9713 GZ, the Netherlands

[2]Department of Biomechanical Engineering, University of Twente, Enschede 7500 AE, The Netherlands

[3]Lead contact

*Correspondence: z.wang01@umcg.nl (Z.W.), v.kalpathyvenkiteswaran@utwente.nl (V.K.V.)

https://doi.org/10.1016/j.xcrp.2025.102614

SUMMARY

Soft robots that respond to externally applied magnetic fields are emerging in various applications with integrated functional materials and patterned magnetization profiles. Current fabrication techniques, such as casting and 3D printing, typically involve prolonged processing cycles, limited throughput, restricted material choices, and substantial challenges in achieving precise, part-specific magnetic programming. Here, we establish a multi-layer screen-printing strategy for directly fabricating the main body of magnetic soft robots with patterned magnetization profiles. Leveraging the inherent advantages of screen-printing, materials such as paper and fabric and rigid substrates including glass and wood can be actuated in magnetic fields to exhibit programmed deformation. By incorporating multiple types of ink and substrate materials, magnetic soft grippers for vascular surgeries, wireless robots with embedded circuitry, and bio-inspired butterfly-like robots are demonstrated. This work improves the functionality and scalability of fabricating magnetic soft robots with expanded potential in deployment across biomedical engineering, robot research, and artistic disciplines.

INTRODUCTION

The emergence of magnetic soft robots (MSRs) has been driven by the development of materials that respond to magnetic fields, enabling programmable magnetization profiles and wireless actuation modes.[1–8] Their untethered and adaptive shape morphing ability enables them to navigate complex environments and perform precise manipulation tasks, providing considerable promise in applications such as health monitoring,[9–12] human-machine interaction,[13,14] and minimally invasive surgery.[15–18] Despite substantial advancements in fabricating MSRs achieved by recent research, integration of various materials and functions with arbitrary pattern and magnetization profiles still remains challenging. A typical approach involves attaching small permanent magnets to the soft robots for magnetic manipulation and localization.[19–22] Alternatively, molding and casting have been the most common fabrication methods utilized for magnetic soft robotics with relatively simple geometry.[23–25] For more complex configurations, a third strategy involves curing composites embedded with magnetizable particles, which are magnetized to saturation in a temporarily deformed state, followed by the manual assembly of components.[26–29] With potential applications in biomedical devices and wearable technologies requiring more consistent and precise fabrication techniques,[30] the limitations of these fabrication methods, particularly in assembly and magnetization processes, have become increasingly evident.

Recognizing these challenges, subsequent advancements in magnetic programming have led to the emergence of more automated methods for fabricating smaller and more delicate structures. Three-dimensional (3D) printing techniques have been developed to create complex 3D architectures that integrate magnetically responsive materials with other functional components.[31–35] However, 3D printing like direct ink writing limits magnetization profiles to a single direction or along the printed fibers, depending on the printer's magnetic system, and photolithography imposes strict requirements on both the materials and the environmental conditions. Recently, heat-assisted reprogramming methods based on phase-change materials with relatively low melting temperature such as polyethylene glycol[36] and polycaprolactone,[37] or heating the magnetic component beyond the Curie temperature and reorienting upon cooling,[38] have been presented for fabricating MSRs. This strategy allows the reorientation of embedded magnetic particles under an external magnetic field above the critical temperature followed by immobilizing the particles through cooling, but it still limits the selection of material systems and the integration of multiple functionalities. All the aforementioned processes require advanced laboratory equipment and materials with specialized physical properties, which significantly elevates the cost for industries to update their production lines. To address the rapidly evolving demands and fulfill the potential of MSRs, it is crucial to develop a simplified and widely applicable fabrication strategy that seamlessly integrates customized magnetization profiles with multifunctional materials.

Screen-printing, a traditional technique with a history spanning over a thousand years, has been one of the most mature and widely adopted methods in various industries, ranging from garment to integrated circuits.[39,40] Through rapid and well-controlled ink transfer, this scheme provides wide pattern flexibility, material adaptability, and high production scalability. At present, screen-printing is prevalent in fabricating soft devices, covering a broad spectrum of applications such as biosensors,[41–43] solar cells,[44–47] and energy storage systems.[48–51] For example, sensors use screen-printed soft electrodes to integrate different sensing modules and simultaneously monitor the key metrics in medical diagnostics.[52,53] Solar cells are developed by screen-printing organic semiconductor thin films that serve as essential components in photovoltaic devices, offering high electrical conductivity and transparency to improve the light-to-electricity conversion efficiency.[54] Screen-printing also simplifies the fabrication of energy storage systems. High-performance electrodes and electrolytes are printed to assemble flexible batteries and supercapacitors.[55,56] The screen-printing approach warrants further investigation due to the comparable rheological properties of magnetic elastomers and traditional viscoelastic inks commonly employed in screen-printing processes. However, research on screen-printing in the direct manufacture of the main body of soft robotics, especially magnetic soft robotics, is limited. We assume that the main resistance comes from the introduction of magnetic programming to printed patterns. In this study, we embrace the screen-printing and magnetic reorientation technique to fabricate and program the main body of magnetic soft robotics, enabling part-specific programming of magnetic polarization. This capability marks a critical step toward scalable, low-cost manufacturing without compromising functional complexity.

Here, a layer-by-layer screen-printing strategy for rapid fabrication of MSRs with customizable magnetization profiles and multiple materials is established (Figure 1). By precisely depositing magnetic ink on elastomer films and other functional substrates, and iteratively programming the orientation of magnetic particles, we create soft robots with responsive shape-morphing ability and other functions. We also present screen-printing of MSRs such as mini-grippers that can navigate in a vascular model and carry small objects wirelessly; programmable surfaces with 3D deformation; multi-layer flexible electronic devices with active deformation modes; and a bio-inspired butterfly robot with fluorescent coloration that responds to ultraviolet (UV) stimuli and flaps in response to magnetic field. Our fabrication scheme provides a platform for producing soft robotic systems, with innovative features such as enhanced versatility, scalability, and functionality, offering prospects for precise, facile, and high-throughput production of MSRs.

RESULTS

Multi-layer screen-printing and magnetic programming

The screen-printing process involves the precise transfer of ink from a stenciled mesh onto the target substrate through three stages: mesh flooding, squeegee action, and separation.[57] In our approach, with the custom screen-printing equipment illustrated in Figure S1 and Video S1, we implement a multi-layer printing technique whereby each subsequent layer is printed with the previous layer as the substrate (see methods for more details). A three-layer printing process is shown in Figure 1A as an example of integrating multiple materials. Initially, a base layer is printed using polysiloxane ink (Figure 1Ai), followed by conductive (or other functional materials) (Figure 1Aii) and magnetic layers (Figure 1Aiii), each formed by carefully controlling the squeegee angle and direction to ensure uniformity. The stenciled mesh is created by attaching laser-scanned, self-adhesive paper to a pre-stretched nylon mesh, which is then secured within a custom 3D-printed frame. Prints with different speeds and mesh sizes are analyzed to further characterize the printing process (Figure S2). The results indicate that, using a 100-mesh screen combined with printing speeds in the range of 10–30 mm/s, yields optimal outcomes, effectively minimizing ink spillage and magnetic particle segregation.

The preparation of the magnetic ink involves blending PrFeB magnetic particles with a polysiloxane elastomer matrix to facilitate magnetic responsiveness and rheological adjustments (Figure 1C). Figure 1D shows the seamless integration of three types of materials and characterized through a scanning electron microscopy (SEM) image (see methods). To optimize the printing quality and magnetic responses, we explore the rheological behavior of non-magnetic ink and magnetic ink through a series of rheology studies (Figure 1E). Steady shearing and oscillatory tests indicate that the mass load and initial magnetization condition of PrFeB particles play a critical role in influencing the magnetic ink's viscosity and viscoelastic properties (see methods). Typically, an increased PrFeB particle ratio enhances both viscosity and viscoelastic properties, while the magnetization of PrFeB particles also shows a pronounced effect on the overall rheological behavior. The ink with magnetized particles shows a high shear-thinning behavior, with a reduction in viscosity as the shear rate increases (Figure 1Ei). The elastic component (storage modulus, G'), is higher than the viscous component (loss modulus, G'') under a relatively low shear strain, where the shear strain of the turning point increases with the mass load of PrFeB particles (Figure 1Eii). This allows the ink to remain stable before and after squeezing but smoothly flow through the mesh. However, an excessively high particle ratio can compromise printing quality due to increased phase inhomogeneity. A mass ratio of 1:1 shows relatively uniform and stable features for both good printing quality and magnetic responses. Figure 1F illustrates the print quality by printing the letters "UMCG," demonstrating the clarity and resolution of the printed pattern. When inks with different mass ratio of magnetic particles were used, the results showed that a low mass ratio led to blurred outlines of the printed pattern, while a high mass ratio caused particle aggregation, clogging the mesh, and resulting in surface defects. The 1:1 mass ratio exhibited the most uniform print quality, with consistent patterning and minimal defects. We use SEM to further characterize the surface of the 1:1 mass ratio sample (Figure 1G). The SEM image reveals a uniform distribution of magnetic particles across the printed surface, which is crucial for confirming the precision and consistency of the screen-printing process.

Please cite this article in press as: Wang et al., Multi-layer screen-printing of magnetic soft robots with integrated materials and functions, Cell Reports Physical Science (2025), https://doi.org/10.1016/j.xcrp.2025.102614

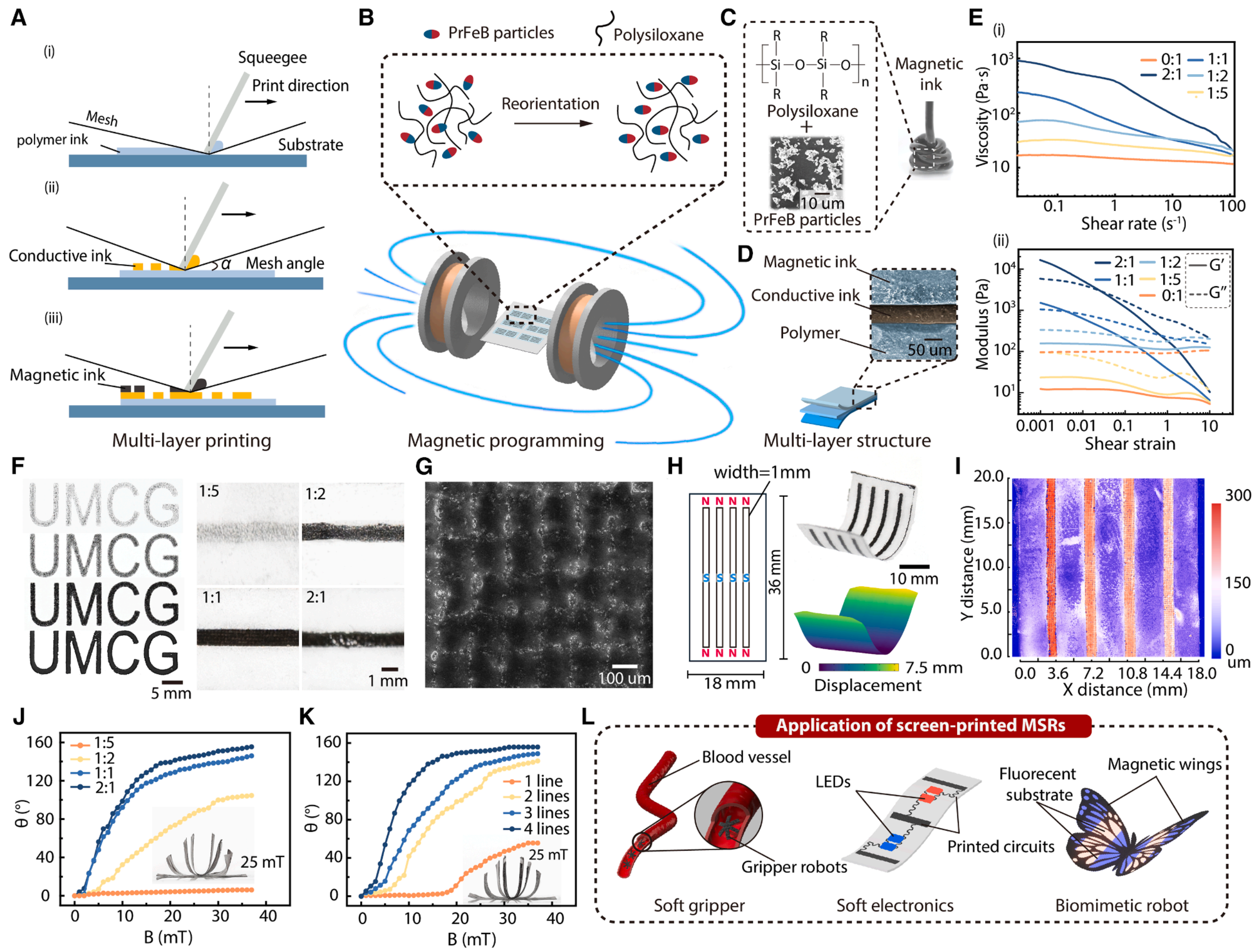

Figure 1. Screen-printing strategy for magnetic soft robotics: process, magnetic customization, material characterization, and applications
(A) Schematic illustration of multi-layer screen-printing process (in roman numeral order).
(B) Magnetic reorientation aligns the magnetic particles in a uniform magnetic field before the polymer matrix curing.
(C) Image of magnetic ink with explanatory diagram of the polymer structure and SEM image of magnetic particles. Scale bar, 10 μm.
(D) Schematic and SEM images of a screen-printed multi-layer sample with the sandwich structure that includes magnetic layer, conductive layer, and polymer layer, respectively. Scale bar, 50 μm.
(E) Rheological properties of magnetic ink with different mass ratio of magnetic particles and filler magnetization conditions.
(F) Printing quality test of magnetic ink with varying mass ratio of particles. Left: printed "UMCG" letters with increasing mass ratio (1:5 to 2:1). Scale bar, 5 mm. Right: magnified views of printed layers showing the impact of mass ratio on layer thickness and uniformity. Scale bar, 1 mm.
(G) SEM image for characterizing the surface morphology and particle distribution on the concentration of the 1:1 sample.
(H) Design and demonstration and finite element analysis simulation of a two-layer prototype bending in the presence of a uniform magnetic field. Scale bar, 10 mm.
(I) Surface morphology test for thickness distribution of a two-layer prototype.
(J) Results of actuation test for two-layer prototypes with 1–4 lines in the magnetic layer.
(K) Results of actuation test for two-layer prototypes with 1:5–2:1 mass ratio.
(L) Schematic illustration for the potential applications of screen-printed magnetic soft robots (MSRs).

To evaluate the print quality and magnetic response, we specifically fabricated a two-layer prototype, which is designed to fold symmetrically in a uniform magnetic field (Figure 1H). The surface morphology of the prototype is examined using a laser scanning morphological system, providing high-resolution topographic details (Figure 1I) (see methods). We then fabricate two-layer prototypes with different numbers of printed lines and subject them to a uniform magnetic field for further evaluating the responsive performance of screen-printed MSRs. As the flux density increases from 0 to 38 mT, the magnetic responsiveness of these devices is quantitatively assessed by measuring θ, the supplementary angle between the two folding edges. The variations in response to the applied magnetic field are recorded and displayed in Figure 1J, offering a detailed comparative analysis of the bending behavior as a function of the number of printed lines. Moreover, another set of prototype samples, each with four printed lines but differing in the mass ratio of magnetic particles of the ink are also evaluated. The results in Figure 1K present the effects of the variations in magnetic ink formulation on magnetic responsiveness and mechanical bending properties.

These experiments establish a robust framework for evaluating and enhancing the printing quality and functional performance of screen-printed MSRs. The detailed analysis of magnetic ink, surface morphology, and magnetic response tests allows us to modify the screen-printing techniques and ink formulations. This, in turn, advances our capability to fabricate MSRs with more realistic functions such magnetic soft grippers, soft robots with onboard electronic circuits and attached LEDs, and biomimetic butterfly robots with fluorescent coloration (Figure 1L).

Screen-printed MSRs with diverse patterns and substrate materials

Currently, soft robots require specialized soft materials (e.g., elastomers, hydrogels) as the main structures. To explore the versatility of the screen-printing technique for magnetic soft robotics on a wide range of surfaces, we employ a series of materials as substrates and perform magnetic actuation on each individual specimen (Figure 2A; Video S2). The selected substrates include natural materials such as wood and cotton fabric, which are assessed for their potential in integrating robotic behaviors with construction materials and wearable technologies; common materials including paper and glass, emphasizing the development of magnetically responsive robots aimed at sustainability and cost-efficiency; and specialized substrates such as indium tin oxide (ITO)-coated films, which are particularly explored for their applications in advanced electronic devices such as perovskite solar cells. Here, we deploy a four-step printing and magnetizing procedure, fabricating two-layer samples for the folding behavior (Figure 2B). After each printing sequence of magnetic ink, the magnetic layer is programmed via magnetic reorientation or impulse magnetizing (Figures 1B and S3) (see methods). Further tensile tests are conducted to characterize the adhesion of printed magnetic soft materials to various substrates. The results show the adhesion strength is sufficient to maintain interface integrity while differences in adhesion still influence the tensile performances of the printed structures (Figure S4).

To validate the potential of our screen-printing method on diverse surfaces, we present a conceptual demonstration highlighting the application of MSRs as foldable solar panels for spacecraft (Figure 2C). Here, a pair of foldable ITO films with screen-printed magnetic actuators is integrated into a satellite model, thereby exhibiting the folding and expanding mechanisms of the MSRs within a space technology context. Figure 2D presents a wireless pH-sensing device fabricated by screen-printing a magnetic actuator between two pH test papers. This device enables wireless testing in environments where manual handling of pH samples is impractical, such as in automated lab-on-a-chip platforms. Screen-printing also substantially reduces the technical and practical barriers to patterning MSRs.

To demonstrate the versatility enabled by screen-printing, we design and present several MSR concepts with 3D shape-morphing structures (Figures 2E and S5; Video S3). These include biomimetic stimuli-responsive mimosa that can fold the leaves under a uniform magnetic field of 20 mT, mimicking the natural closing motion of *Mimosa pudica* in response to external stimuli. Additionally, we show an origami-inspired soft robot consisting of a flexible sheet that deforms into a cube actuated via a magnetic field generated by a permanent magnet, demonstrating the potential for complex shape transformations and the creation of reconfigurable structures through magnetic actuation facilitated by screen-printing. Furthermore, we introduce an undulating ring structure with eight pairs of arrow-shaped actuators, where each arrow is magnetized in the direction indicated by the printed pattern, highlighting the ability to program complex deformation modes into MSRs. These demonstrations indicate that our screen-printing approach can endow MSRs with a diverse range of patterns and deformation modes for future applications.

The development of dynamically shape-morphing soft surfaces that can perform precise and real-time reshaping behavior driven by magnetic fields is pivotal in soft robotics.[58] In Figure 2F, we demonstrate the fabrication of screen-printed magnetic soft surfaces with programmable shape-morphing capabilities. The process begins with printing a layer of non-magnetized polysiloxane grid, which serves as the substrate. Subsequent layers involve depositing magnetic ink at specifically designed nodes, which are then magnetized to achieve programmed rotational movements (Figure S6). By strategically arranging these magnetic nodes, we create three distinct magnetic programmable surfaces that exhibit different shape-morphing scenarios: single polar (shape I), dual polar (shape II), and saddle-shaped surfaces (shape III), also demonstrated in Video S4. Screen-printing of programmable surfaces enables autonomous systems to have adaptive shape morphing, thereby expanding the potential applications of soft robotics in fields requiring dynamic surface transformations.

Screen-printing of magnetic soft gripper robots

Soft gripper robots have garnered widespread interest due to their unique combination of flexibility, adaptability, and precision. These robots are particularly advantageous in biomedical applications, where their soft, compliant nature allows for delicate interactions with biological tissues.[59] The integration of magnetic materials facilitates remote actuation, enabling maneuvers without invasive intervention. Current advancements have primarily achieved progress in materials and controls, where scalable methods for fabricating gripper robots have received comparatively less attention.[60]

In this study, we employed the screen-printing technique to realize fast prototyping and functional integration potential of magnetic soft gripper robots (MSGRs) for biomedical applications. Figure 3A shows the geometry and magnetization profile of the grippers, where the six beams are radially magnetized (Figure S7). The gripper robots have two deformation modes: folding and expansion, as illustrated and simulated in Figure 3C. To fabricate the MSGRs, magnetic ink is printed on an acrylic substrate through a stenciled mold, which allows for fabricating 100 grippers within a 40 $\times$ 40 mm area by a single squeegeeing (Figure 3D).

Cell Reports
Physical Science
Article

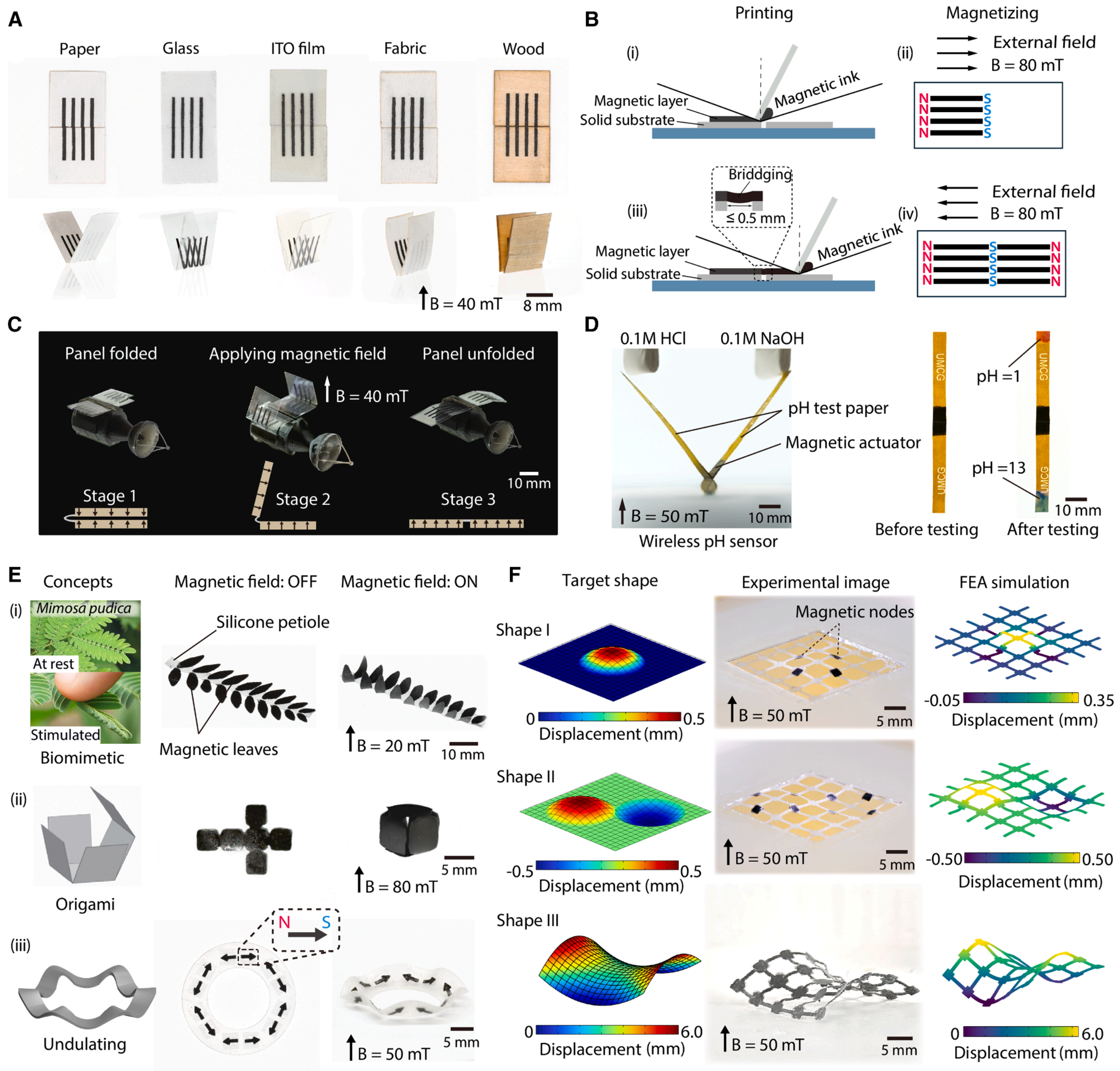

Figure 2. Broad adaptability of screen-printing magnetic soft robotics onto various substrates and their pattern functionality

(A) Screen-printed foldable samples with different substrate materials. Each sample shows a folding deformation under a uniform magnetic field of 40 mT. Scale bar, 8 mm.

(B) Schematic diagram of screen-printing and reorientation steps (in roman numeral order).

(C) Demonstration of using ITO films as substrate materials for screen-printed magnetically foldable solar panels in space engineering. Scale bar, 10 mm.

(D) Demonstration of wireless pH sensor device that simultaneously tests the pH value of two samples by magnetically folding pH test papers, where a single layer of magnetic soft material is printed as the hinge. Scale bars, 10 mm.

(E) Demonstration of three concepts with 3D shape-morphing structures: (i) biomimetic design of stimuli-responsive mimosa leaves, which can fold under a uniform magnetic field. Scale bar, 10 mm. (ii) Origami-inspired design of a foldable sheet that deforms into a cube in the presence of a magnetic field. Scale bar, 5 mm. (iii) An undulating ring structure with eight pairs of arrow-shaped actuators, where each arrow is magnetized in the direction indicated by the pattern. Scale bar, 5 mm.

(F) Magnetic programmable surfaces with precise shape-morphing ability, color bars, displacement on vertical direction. Scale bars, 10 mm.

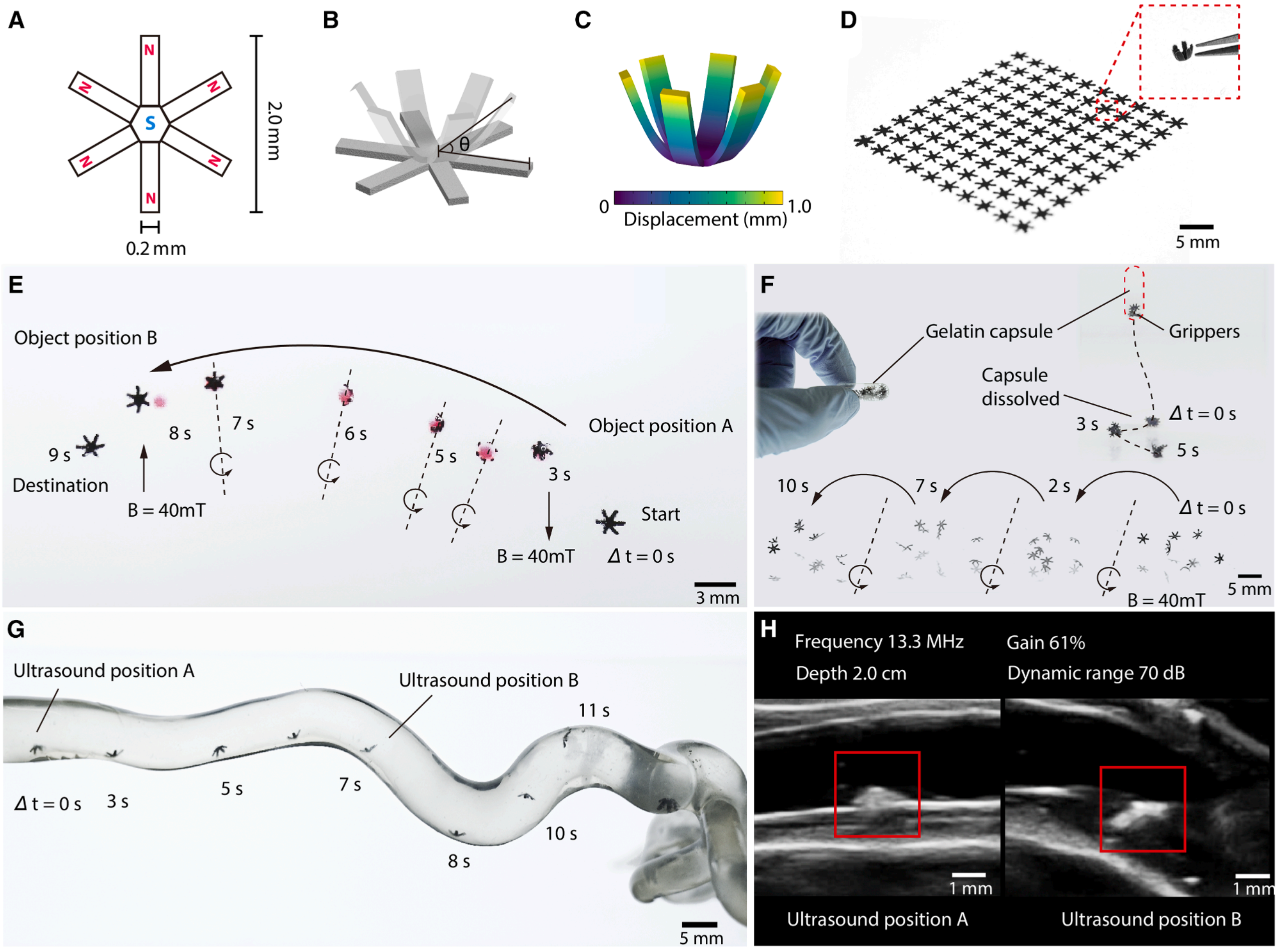

Figure 3. Screen-printed magnetic soft gripper robots

(A) Geometric design and magnetic configuration (as detailed in Figure S7) of the gripper robots.

(B) Schematic illustration of magnetic soft gripper being actuated in the presence of a magnetic field.

(C) Finite element analysis simulation for the magnetic gripper robot placed in a uniform magnetic field of 60 mT.

(D) Image of 100 grippers fabricated with a single squeegee. The inset shows a gripper actuated by a uniform magnetic field of 60 mT. Scale bar, 5 mm.

(E) Rolling-based locomotion of a gripper robot for sphere-shaped cargo transport under a rotating magnetic field. Scale bar, 3 mm.

(F) Demonstration of a capsule-based robot delivery strategy, with 25 gripper robots sealed in a gelatin capsule. After the capsule dissolves in water, the gripper robots are actuated to escape and perform group locomotion under a rotating magnetic field generated by a permanent magnet. Scale bar, 5 mm.

(G) Demonstration of the gripper robot navigating in a trigeminal artery model using rolling-based locomotion under a rotating magnetic field generated by a permanent magnet. Scale bar, 5 mm.

(H) Ultrasound tracking image of the gripper robots while navigating in the trigeminal artery model. Scale bar, 1 mm.

The grippers are deployed as drug delivery robots in a scenario that replicates motion inside the fluid environment of the human body (Figure 3E; Video S5). The programmed magnetization profile of the MSGRs also allows for rolling-based locomotion when placed in a rotating magnetic field. Meanwhile, the gripper's folding deformation can firmly grasp and release the object with up to 200% of its body weight. Additionally, the small size and wireless actuation of MSGRs allow them to be packaged in a dissolvable capsule, from which 20 gripper robots were released and manipulated to break free (Figure 3F; Video S6). The escaped gripper robots simultaneously respond to the actuation magnetic field that allows for controllable group behavior. We further explored the potential application of screen-printed MSGRs in minimally invasive surgery. As illustrated in Figure 3G and Video S7, the MSGR is actuated to navigate in a trigeminal artery model. We set up ultrasound imaging to validate the real-time tracking potential of the MSGRs, where the ultrasound imaging results show a clear outline and movements of the gripper robots at a depth of 2.0 cm. These results demonstrate the advantages afforded by screen-printing of MSGRs, highlighting the high throughput and reliability of fabrication at small sizes.

Multi-modal MSRs embedded with onboard circuitry

Flexible electronic devices are increasingly valued in biomedical sciences due to their mechanical compliance with tissue and

Please cite this article in press as: Wang et al., Multi-layer screen-printing of magnetic soft robots with integrated materials and functions, Cell Reports Physical Science (2025), https://doi.org/10.1016/j.xcrp.2025.102614

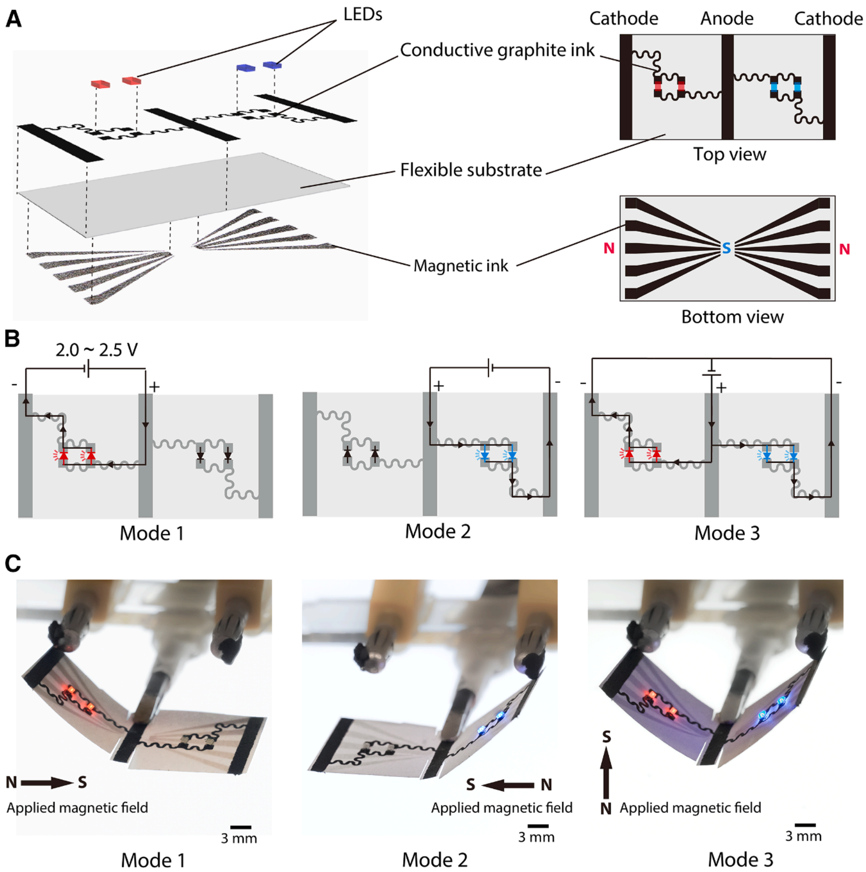

Figure 4. Schematic designs and working principles of the screen-printed flexible electronic device

(A) Exploded, top, and bottom view of the flexible electronic device, in which flexible electronic circuitry and magnetic actuators are embedded based on screen-printing. Scale bar, 3 mm.

(B) Schematic diagram of the embedded flexible electronic circuits, which are designed to turn on only in the designated mode of transformation owing to the selective contact with the electrode on the substrate. Scale bar, 3 mm.

(C) Images of the screen-printed flexible electronic device activated by magnetic fields in different directions with the same magnitude of 80 mT. Scale bar, 3 mm.

organs, providing more conformal contact and higher efficient transmission of electrical, optical, and mechanical signals. Recently, magnetic soft materials have enabled the creation of magnetically reconfigurable soft or flexible electronic devices with embedded electronic components, achieved through molding or 3D printing.[61,62] These devices can perform different electronic functions through shape morphing under applied magnetic fields, featuring dynamic adaptability in electronic performance.

Current fabrication methods require producing a complete MSR before assembling the circuits, limiting the fabrication efficiency and inter-layer integration. To overcome the limits, we have employed the screen-printing strategy to enable the simultaneous printing of both circuits and actuation modules, offering advantages in versatility, efficiency, and the seamless integration of multi-modal functionalities. The layered architecture resulting from this process is illustrated in Figure 4A, which presents a flexible electronic device wherein flexible electronic circuitry and magnetic actuators are embedded using screen-printing. A flexible paper-based substrate serves as the structural layer, selected for its superior compatibility with both magnetic and conductive inks. As illustrated in Figure 4B, the embedded flexible electronic circuits are intricately patterned using conductive graphite ink (see methods). This configuration incorporates two LED modules to exhibit three distinct illumination modes, which are achievable through connections to circuit terminals. The circuits are designed to activate only in the corresponding mode of deformation, owing to the selective contact with the electrode on the substrate. Subsequently, magnetic ink is printed on the reverse side of the substrate and subjected to magnetization. Figure 4C and Video S8 exhibit the screen-printed flexible electronic device to illustrate the activation modes under magnetic fields of identical magnitude (80 mT) applied in different directions. Specifically, under a horizontal left magnetic field, folding of the left-sided panel activates the red LEDs, and folding of the right-sided panel activates the blue LED while placed in a magnetic field in opposite direction. A vertical upward field induces upward bending with all LEDs illuminated. The seamless integration of heterogeneous materials and components highlights the potential of screen-printed MSRs to advance future flexible electronics with multi-layer structures.

Bio-inspired MSR with fluorescent coloration

Inspired by natural organisms, biomimetic robots replicate specific structural and functional features of living creatures, enabling innovative solutions tailored to complex challenges. For instance, their ability to emulate natural locomotion and adaptive behaviors offers practical advantages in tasks such as targeted drug delivery, dynamic environmental monitoring, and interactive educational tools.[29,63] The designs inspired by a variety of creatures, including those observed in snakes, inchworms, birds, jellyfish, spermatozoa, and turtles, have emerged as a prominent research area in soft robotics. Inspired by butterflies' appearance (Figure 5A), along and their efficient flapping motion, we have designed MSRs with a butterfly pattern and flapping behavior. The flapping of the wings is achieved by screen-printing and reorientating magnetic layers on top of polysiloxane substrates (Video S9).

Biofluorescence is a phenomenon where living organisms absorb electromagnetic radiation at a specific wavelength and emit it at a lower energy level and a longer wavelength, playing

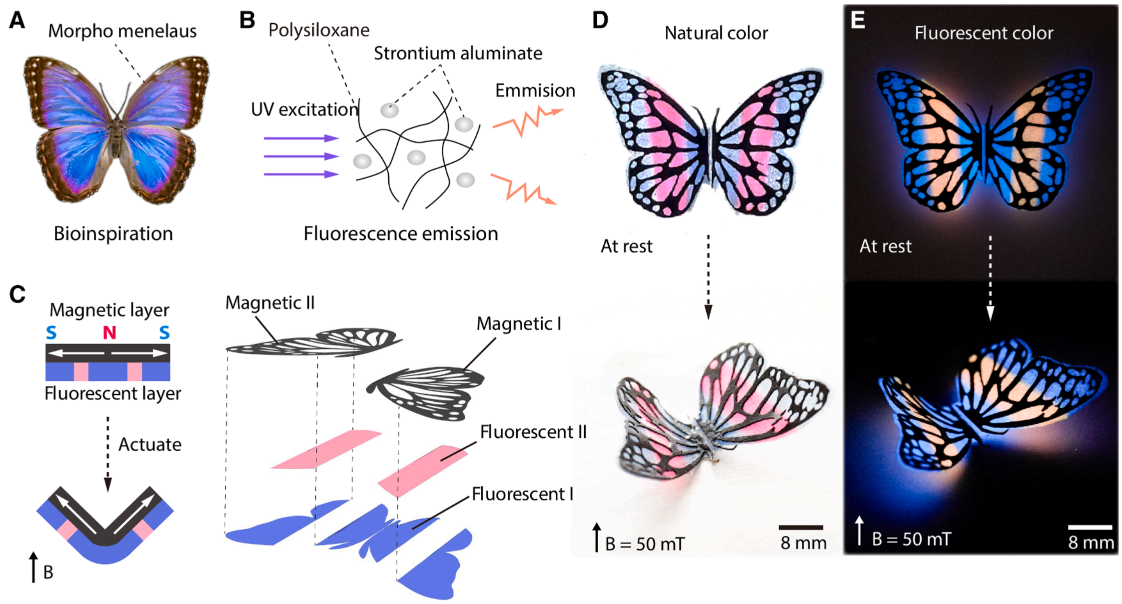

Figure 5. Bio-inspired butterfly robot with fluorescent coloration

(A) Image of the butterfly (*Morpho menelaus*) for bioinspiration.

(B) Fluorescence afterglow emission mechanism of fluorescent ink.

(C) Schematic illustration of the layer structure and actuation mode of screen-printed butterfly robot.

(D) Screen-printed butterfly robot at rest and being actuated when placed in natural light. Scale bar, 8 mm.

(E) Screen-printed butterfly robot at rest and being actuated after being excited by ultraviolet (UV) light (wavelength ~410 nm). Scale bar, 8 mm.

an important role in camouflage, threat display, and attraction.[64,65] The integration of fluorescent materials in bio-inspired robots endows more realism, enabling visual feedback and enhancing the esthetic appeal of soft robots. We create fluorescent ink for screen-printing by mixing polysiloxane with strontium aluminate glow powder, which can be excited by UV light and emits visible afterglow (Figures 5B and S6) (see methods). The butterfly robot is constructed through a strategic layering of fluorescent ink and magnetic ink (Figure 5C). The magnetic layer is polarized with alternating poles (S-N-S configuration), which enables wing flapping of the butterfly when exposed to an actuating magnetic field. Specifically, we establish the structure through a four-layer printing procedure to integrate the fluorescent layer with magnetic actuators while each layer is illustrated in the exploded schematic of Figure 5C. We further demonstrate the magnetic butterfly robot's response under both natural and fluorescent color conditions. In Figure 5D, the robot is shown in its natural color, both at rest and during actuation under a uniform magnetic field of 50 mT. In Figure 5E and Video S9, the robot displays its fluorescent color, with a distinct afterglow observed following UV excitation (wavelength, ~410 nm), highlighting its luminescent properties. These functionalities operate in parallel rather than interactively, their simultaneous yet independent operation is an important achievement, highlighting the compatibility and non-interference between magnetically and optically responsive systems. Fluorescent coloration, activated externally by UV exposure, provides a stand-alone visual functionality ideal for bioimaging or environmental sensing. Meanwhile, independent magnetic actuation enables precise shape morphing. This decoupled design approach ensures modularity, allowing each functional system to be individually optimized and adapted for a wide range of applications. This combined concept of screen-printed MSR exemplifies the potential for integrating esthetics and functionality into soft robotic systems, broadening application prospects in biomedical imaging, and educational robots.

DISCUSSION

In this study, we have introduced a screen-printing-based multilayer fabrication scheme for magnetic soft robotics. This method harnesses the unique advantages of screen-printing, including broad applicability across various materials and patterns, as well as layering, which seamlessly integrates distinct functional layers. We have demonstrated a precise deposition process and improved the printability of magnetic ink with a high filler ratio (50 wt %) and stable rheological properties. The comprehensive material applicability of the screen-printing method has been verified by successfully printing on diverse substrates and actuating in magnetic fields. We also applied the multistep magnetization procedure to customize the magnetic responses. The screen-printing technique is demonstrated through various examples, including biomimetic mimosa leaves, origami cubes, undulating rings, and reconfigurable surfaces, all capable of programmable 3D shape morphing. Building upon these demonstrations, three advanced applications are showcased: tether-free gripper robots designed for biomedical purposes, fully printed three-layer soft robots integrated with onboard circuits for actuatable flexible electronics, and a bio-inspired butterfly robot featuring fluorescent coloration. Collectively, these examples underscore screen-printing's versatility and potential for creating functional MSRs with diverse capabilities. Despite these strengths, inherent limitations exist in fabricating fully 3D freeform architectures with screen-printing. Compared with extrusion-based 3D printing methods such as direct ink writing and fused filament fabrication, screen-printing typically restricts the thickness of the designs to a few tenths of a millimeter and limits the bridging distances achievable. Nonetheless, screen-printing excels in applications demanding exceptional planar resolution, rapid prototyping, and scalable production of 2D and 2.5D structures. These unique capabilities position screen-printing as a promising method for mass production and functional integration, particularly suited to automation industries, biomedical devices, and educational settings.

While the screen-printing strategy is demonstrated to be a noteworthy advance for the fabrication of MSRs with silicone mixtures, we propose further exploration of water-based material systems, including hydrogels and other dispersions, to elevate the integration of the screen-printed MSRs in high-demand applications such as minimally invasive surgery and tissue engineering. Such efforts could involve investigating alternative water-based ink matrices that exhibit optimized rheological properties, stable boundary attachment, and robust mechanical performance. Furthermore, due to magnetic reorientation, the strategy inherently supports batch programming, enabling simultaneous magnetization of multiple robot components sharing identical polarization directions in a single step. Future automation could involve incorporating conveyor belt-based magnetic programming stations or programmable magnet arrays, streamlining mass production and enabling rapid, high-throughput manufacturing of MSRs. Developing an automatic configuration algorithm that converts the demanded deformation modes to simple printing and magnetic reorientation sequences is also important in the future automation. These explorations would significantly broaden the adaptability and functionality of soft robotics. We envision that the screen-printing of MSRs could provide a foundation for untethered soft robots and flexible electronics, enabling their deployment in diverse biomedical and industrial applications while advancing scalable and cost-effective manufacturing methods.

METHODS

Ink preparation

Magnetic ink preparation

To prepare the magnetic ink, we utilized a composite system consisting of magnetic particles and elastomers. Magnetic particles (PrFeB, MQFPTM-16-7) were selected due to their high magnetic remanence. Before mixing, all the PrFeB particles were magnetized beyond saturation using an impulse magnetizer (IM-10-30, ASC Scientific). The elastomer matrix, Dragon Skin 30 (Smooth-On), was prepared by mixing silicone resin and curing agent at a 1:1 weight ratio. The PrFeB particles were gradually added to the matrix at a 1:1 weight ratio, and the entire formulation was blended by an overhead stirrer (NANOSTAR, IKA, Germany) at ~2,000 rpm for 2 min to ensure homogeneity. The final mixture was degassed for 5 min in a vacuum chamber to eliminate air bubbles.

Conductive ink preparation

The conductive ink is prepared by mixing Electric Paint (Bare Conductive, UK) with glycerin (Glycerol, Sigma-Aldrich) in a volume ratio of 100:1. The final mixture was degassed for 5 min in a vacuum chamber to eliminate air bubbles.

Fluorescent ink preparation

Strontium aluminate-based glowing powder (purchased from Alibaba, China) was blended with Dragon Skin 30 (Smooth-On) in a volume ratio of 1:1. The final mixture was degassed for 5 min in a vacuum chamber to eliminate air bubbles. The images of fluorescent ink before and after UV excitation are shown in Figure S8.

Screen-printing procedures

The MSRs were fabricated using a layer-by-layer screen-printing technique. A piece of 120 mesh nylon net with a laser-cut screen was tensed and mounted onto a 3D-printed frame (Figure S1). Each layer of magnetic ink was deposited by sweeping an acrylic squeegee at an angle of around 70° and a manually controlled pressure. The substrates, including elastomer films, paper, glass, and wood, were secured onto the printing stage. After printing each layer, the ink was cured at 80°C for 10 min on a heating platform. For multi-layered devices, additional layers were printed following the same procedure.

Magnetic programming

We employed two magnetic programming methods in this research to streamline the fabrication process, depending on the requirements of specific samples. These methods are described in detail in Figure S3 and Table S1. The majority of samples are programmed by magnetic reorientation, as demonstrated in our previous research,[66] where particles are aligned in a relatively weak magnetic field. Each alignment sequence required approximately 5 s within a pair of electromagnetic coils at a magnetic induction intensity of 80 mT. After alignment, each programmed region was cured at 100°C for 30 s.

For more complex structures, such as the origami cube (Figure 2E) and gripper robots (Figure 3), we applied magnetization by an impulse magnetizer (IM-10-30, ASC Scientific). The samples were first fixed to deform in an acrylic mold and magnetized in the impulse magnetizer for less than 1 s under a strong magnetic field of 2.5 T. This method was chosen because these designs require stronger magnetic responses and multiple directional alignments, which would necessitate repeated printing cycles if using magnetic reorientation, thus potentially compromising positional accuracy.

Rheological test

The rheological properties of the magnetic ink were measured using a rotational rheometer (Anton Paar MCR 302). The ink was loaded onto the parallel plate fixture with a 25 mm diameter at a 1 mm gap. A shear rate sweep was performed from 0.01 to 1,000 s^{-1} at room temperature to determine the ink's viscosity profile and shear-thinning behavior, crucial for the screen-printing process. Additionally, oscillatory tests were conducted to measure the storage modulus (G′) and loss modulus (G″) at a constant frequency of 1 Hz, providing insights into the viscoelastic properties of the ink.

Surface morphology test

The surface morphology test in Figure 1I was analyzed using a two-axis morphology meter (Scantron Industrial Proscan 2000, UK). The sample was scanned by a laser sensor in the *Y* direction with 0.01 mm accuracy. The data were processed by R version 4.3.1 to generate the contour plot.

SEM characterization

SEM (Thermo Fisher Apreo S) was used to examine the morphologies and mesoscopic structures of the printed film. The sample was spread flat and securely affixed to the test bench before SEM characterization and analyzed at an accelerating voltage of 10 kV. This characterization allowed us to observe the printing quality and dispersion of the magnetic particles in the elastomer matrix.

Finite element analysis

For the designs presented in Figures 1H, 2F, and 3C, deformations in the presence of external magnetic fields were simulated using the Solid Mechanics and Magnetic Fields, No Currents (mfnc) module in COMSOL Multiphysics 5.4. Materials and environmental parameters are listed in Table S2.

Material mechanical characterization

The tensile tests are conducted using a texture analyzer (CT3, AMETEK Brookfield). Standardized testing samples made of Dragon skin 30 and the magnetic composites are subjected to axis tensile tests as per ASTM standard tests. The loading speed for the tests is set to 1 mm/s, and the testing range is set to 200% strain. Nominal stress-strain curves are provided in Figure S9.

RESOURCE AVAILABILITY

Lead contact

Further information and requests for resources should be directed to and will be fulfilled by the lead contact, Zhuoyue Wang (z.wang01@umcg.nl).

Materials availability

This study did not generate new unique materials.

Data and code availability

- The data supporting this study are available in the manuscript and supplemental information.
- This paper does not report any original code.
- Any additional information required to reanalyze the data reported in this paper is available from the lead contact upon request.

ACKNOWLEDGMENTS

We thank J. Hu for plotting Figure 1I and C. Li for providing the artery model and technical support on ultrasound imaging. This work was partly financially supported by the Europe Research Council (ERC) European Union's Horizon 2020 Research and Innovation program (no. 866494-project MAESTRO) and China Scholarship Council (CSC) (file no. 202106180026).

AUTHOR CONTRIBUTIONS

Conceptualization, Z.W. and V.K.V.; methodology, Z.W., V.K.V., and S.M.; visualization, Z.W. and V.K.V.; funding acquisition, S.M. and Z.W.; supervision, V.K.V. and S.M.; writing – original draft, Z.W.; writing – review & editing, Z.W., V.K.V., and S.M.

DECLARATION OF INTERESTS

The authors declare no competing interests.

SUPPLEMENTAL INFORMATION

Supplemental information can be found online at https://doi.org/10.1016/j.xcrp.2025.102614.

Received: January 27, 2025
Revised: April 7, 2025
Accepted: May 7, 2025
Published: June 4, 2025

REFERENCES

1. Rahmer, J., Stehning, C., and Gleich, B. (2017). Spatially selective remote magnetic actuation of identical helical micromachines. Sci. Robot. *2*, eaal2845.
2. Xu, T., Zhang, J., Salehizadeh, M., Onaizah, O., and Diller, E. (2019). Millimeter-scale flexible robots with programmable three-dimensional magnetization and motions. Sci. Robot. *4*, eaav4494.
3. Kwok, S.W., Morin, S.A., Mosadegh, B., So, J.H., Shepherd, R.F., Martinez, R.V., Smith, B., Simeone, F.C., Stokes, A.A., and Whitesides, G.M. (2014). Magnetic Assembly of Soft Robots with Hard Components. Adv. Funct. Mater. *24*, 2180–2187. https://doi.org/10.1002/ADFM.201303047.
4. Wang, Z., Li, W., Klingner, A., Pei, Y., Misra, S., and Khalil, I.S.M. (2024). Magnetic control of soft microrobots near step-out frequency: Characterization and analysis. Comput. Struct. Biotechnol. J. *25*, 165–176. https://doi.org/10.1016/J.CSBJ.2024.08.022.
5. Cui, J., Huang, T.Y., Luo, Z., Testa, P., Gu, H., Chen, X.Z., Nelson, B.J., and Heyderman, L.J. (2019). Nanomagnetic encoding of shape-morphing micromachines. Nature *575*, 164–168. https://doi.org/10.1038/s41586-019-1713-2.
6. Han, M., Guo, X., Chen, X., Liang, C., Zhao, H., Zhang, Q., Bai, W., Zhang, F., Wei, H., Wu, C., et al. (2022). Submillimeter-scale multimaterial terrestrial robots. Sci. Robot. *7*, eabn0602.
7. Xu, C., Faul, C.F.J., Taghavi, M., and Rossiter, J. (2023). Electric Field-Driven Dielectrophoretic Elastomer Actuators. Adv. Funct. Mater. *33*, 2208943. https://doi.org/10.1002/ADFM.202208943.
8. Li, Z., Zhang, S., Wang, Q., Xu, Y., Li, Y., Chen, X., Chen, P., Chen, D., Shi, Y., and Su, B. (2024). Untethered & Stiffness-Tunable Ferromagnetic Liquid Robots for Cleaning Thrombus in Complex Blood Vessels. Adv. Mater. *36*, 2409142. https://doi.org/10.1002/ADMA.202409142.
9. Yang, H., Li, S., Wu, Y., Bao, X., Xiang, Z., Xie, Y., Pan, L., Chen, J., Liu, Y., and Li, R.W. (2024). Advances in Flexible Magnetosensitive Materials and Devices for Wearable Electronics (Preprint at John Wiley and Sons Inc). https://doi.org/10.1002/adma.202311996.
10. Li, Y., Chen, Z., Zheng, G., Zhong, W., Jiang, L., Yang, Y., Jiang, L., Chen, Y., and Wong, C.P. (2020). A magnetized microneedle-array based flexible triboelectric-electromagnetic hybrid generator for human motion monitoring. Nano Energy *69*, 104415. https://doi.org/10.1016/J.NANOEN.2019.104415.
11. Yan, G., Solovev, A.A., Huang, G., Cui, J., and Mei, Y. (2022). Soft microswimmers: Material capabilities and biomedical applications. Curr. Opin. Colloid Interface Sci. *61*, 101609. https://doi.org/10.1016/J.COCIS.2022.101609.

12. Wu, Y., Cai, L., Li, Z., Chen, G., Maharjan, S., He, M., and Su, B. (2025). Autonomous Self-Healing Magnetoelectric I-Skin from Self-Bonded Deep Eutectic Polymer. Small Methods, 2402190. https://doi.org/10.1002/SMTD.202402190.

13. Yin, R., Wang, D., Zhao, S., Lou, Z., and Shen, G. (2021). Wearable Sensors-Enabled Human–Machine Interaction Systems: From Design to Application. Adv. Funct. Mater. *31*, 2008936. https://doi.org/10.1002/adfm.202008936.

14. Zhang, H., Zhang, D., Wang, Z., Xi, G., Mao, R., Ma, Y., Wang, D., Tang, M., Xu, Z., and Luan, H. (2023). Ultrastretchable, Self-Healing Conductive Hydrogel-Based Triboelectric Nanogenerators for Human-Computer Interaction. ACS Appl. Mater. Interfaces *15*, 5128–5138.

15. Richter, M., Kaya, M., Sikorski, J., Abelmann, L., Kalpathy Venkiteswaran, V., and Misra, S. (2023). Magnetic Soft Helical Manipulators with Local Dipole Interactions for Flexibility and Forces. Soft Robot. *10*, 647–659.

16. Kim, Y., Parada, G.A., Liu, S., and Zhao, X. (2019). Ferromagnetic soft continuum robots. Sci. Robot. *4*, eaax7329. https://doi.org/10.1126/scirobotics.aax7329.

17. Liu, J., Yu, S., Xu, B., Tian, Z., Zhang, H., Liu, K., Shi, X., Zhao, Z., Liu, C., Lin, X., et al. (2021). Magnetically propelled soft microrobot navigating through constricted microchannels. Appl. Mater. Today *25*, 101237. https://doi.org/10.1016/J.APMT.2021.101237.

18. Torlakcik, H., Sevim, S., Alves, P., Mattmann, M., Llacer-Wintle, J., Pinto, M., Moreira, R., Flouris, A.D., Landers, F.C., Chen, X.Z., et al. (2024). Magnetically Guided Microcatheter for Targeted Injection of Magnetic Particle Swarms. Adv. Sci. *11*, 2404061. https://doi.org/10.1002/ADVS.202404061.

19. Li, C., Misra, S., and Khalil, I.S.M. (2023). Navigation of Untethered Small-Scale Helical Devices Using Magnetic System under Ultrasound Guidance. IEEE Trans. Med. Robot. Bionics *5*, 1093–1104. https://doi.org/10.1109/TMRB.2023.3318642.

20. Heunis, C.M., Wang, Z., de Vente, G., Misra, S., and Venkiteswaran, V.K. (2023). A Magnetic Bio-Inspired Soft Carrier as a Temperature-Controlled Gastrointestinal Drug Delivery System. Macromol. Biosci. *23*, e2200559. https://doi.org/10.1002/mabi.202200559.

21. Miyashita, S., Guitron, S., Li, S., and Rus, D. (2017). Robotic metamorphosis by origami exoskeletons. Sci. Robot. *2*, eaao4369.

22. Gu, H., Boehler, Q., Ahmed, D., and Nelson, B.J. (2019). Magnetic quadrupole assemblies with arbitrary shapes and magnetizations. Sci. Robot. *4*, eaax8977. https://doi.org/10.1126/SCIROBOTICS.AAX8977.

23. Lum, G.Z., Ye, Z., Dong, X., Marvi, H., Erin, O., Hu, W., and Sitti, M. (2016). Shape-programmable magnetic soft matter. Proc. Natl. Acad. Sci. USA *113*, E6007–E6015.

24. Jackson, J.A., Messner, M.C., Dudukovic, N.A., Smith, W.L., Bekker, L., Moran, B., Golobic, A.M., Pascall, A.J., Duoss, E.B., Loh, K.J., and Spadaccini, C.M. (2018). Field responsive mechanical metamaterials. Sci. Adv. *4*, eaau6419.

25. Wang, C., Puranam, V.R., Misra, S., and Venkiteswaran, V.K. (2022). A Snake-Inspired Multi-Segmented Magnetic Soft Robot Towards Medical Applications. IEEE Robot. Autom. Lett. *7*, 5795–5802. https://doi.org/10.1109/LRA.2022.3160753.

26. Zhang, J., Ren, Z., Hu, W., Soon, R.H., Yasa, I.C., Liu, Z., and Sitti, M. (2021). Voxelated three-dimensional miniature magnetic soft machines via multimaterial heterogeneous assembly. Sci. Robot. *6*, eabf0112. https://doi.org/10.1126/SCIROBOTICS.ABF0112.

27. Hu, W., Lum, G.Z., Mastrangeli, M., and Sitti, M. (2018). Small-scale soft-bodied robot with multimodal locomotion. Nature *554*, 81–85. https://doi.org/10.1038/nature25443.

28. Wang, C., Mzyk, A., Schirhagl, R., Misra, S., and Venkiteswaran, V.K. (2023). Biocompatible Film-Coating of Magnetic Soft Robots for Mucoadhesive Locomotion. Adv. Mater. Technol. *8*, 2201813. https://doi.org/10.1002/ADMT.202201813.

29. Venkiteswaran, V.K., Samaniego, L.F.P., Sikorski, J., and Misra, S. (2019). Bio-Inspired Terrestrial Motion of Magnetic Soft Millirobots. IEEE Robot. Autom. Lett. *4*, 1753–1759. https://doi.org/10.1109/lra.2019.2898040.

30. Kim, Y., and Zhao, X. (2022). Magnetic Soft Materials and Robots. Chem. Rev. *122*, 5317–5364. https://doi.org/10.1021/ACS.CHEMREV.1C00481.

31. Lee, H., Jang, Y., Choe, J.K., Lee, S., Song, H., Lee, J.P., Lone, N., and Kim, J. (2020). 3D-printed programmable tensegrity for soft robotics. Sci. Robot. *5*, eaay9024. https://doi.org/10.1126/SCIROBOTICS.AAY9024.

32. Khalid, M.Y., Arif, Z.U., Tariq, A., Hossain, M., Ahmed Khan, K., and Umer, R. (2024). 3D printing of magneto-active smart materials for advanced actuators and soft robotics applications. Eur. Polym. J. *205*, 112718. https://doi.org/10.1016/J.EURPOLYMJ.2023.112718.

33. Zhang, Y., Pan, C., Liu, P., Peng, L., Liu, Z., Li, Y., Wang, Q., Wu, T., Li, Z., Majidi, C., and Jiang, L. (2023). Coaxially printed magnetic mechanical electrical hybrid structures with actuation and sensing functionalities. Nat. Commun. *14*, 4428. https://doi.org/10.1038/S41467-023-40109-Z.

34. Sanchis-Gual, R., Ye, H., Ueno, T., Landers, F.C., Hertle, L., Deng, S., Veciana, A., Xia, Y., Franco, C., Choi, H., et al. (2023). 3D Printed Template-Assisted Casting of Biocompatible Polyvinyl Alcohol-Based Soft Microswimmers with Tunable Stability. Adv. Funct. Mater. *33*, 2212952. https://doi.org/10.1002/ADFM.202212952.

35. Zhang, S., Xu, Y., Li, Z., Li, Y., Lu, Z., Chen, X., Chen, P., Chen, M., Zhang, P., Cai, C., et al. (2024). Ultra-Fast Shape-Deformation and Highly-Sensitive Detection of 4D Printed Electromagnetic Architectures. Adv. Funct. Mater. *34*, 2402563. https://doi.org/10.1002/ADFM.202402563.

36. Song, H., Lee, H., Lee, J., Choe, J.K., Lee, S., Yi, J.Y., Park, S., Yoo, J.W., Kwon, M.S., and Kim, J. (2020). Reprogrammable Ferromagnetic Domains for Reconfigurable Soft Magnetic Actuators. Nano Lett. *20*, 5185–5192.

37. Deng, H., Sattari, K., Xie, Y., Liao, P., Yan, Z., and Lin, J. (2020). Laser reprogramming magnetic anisotropy in soft composites for reconfigurable 3D shaping. Nat. Commun. *11*, 6325. https://doi.org/10.1038/s41467-020-20229-6.

38. Alapan, Y., Karacakol, A.C., Guzelhan, S.N., Isik, I., and Sitti, M. (2020). Reprogrammable shape morphing of magnetic soft machines. Sci. Adv. *6*, eabc6414. https://doi.org/10.1126/sciadv.abc6414.

39. Chen, C., Ran, C., Yao, Q., Wang, J., Guo, C., Gu, L., Han, H., Wang, X., Chao, L., Xia, Y., and Chen, Y. (2023). Screen-Printing Technology for Scale Manufacturing of Perovskite Solar Cells. Adv. Sci. *10*, 2303992. https://doi.org/10.1002/ADVS.202303992.

40. Kapur, N., Abbott, S.J., Dolden, E.D., and Gaskell, P.H. (2013). Predicting the Behavior of Screen Printing. IEEE Trans. Compon. Packaging Manuf. Technol. *3*, 508–515. https://doi.org/10.1109/TCPMT.2012.2228743.

41. Taleat, Z., Khoshroo, A., and Mazloum-Ardakani, M. (2014). Screen-printed electrodes for biosensing: A review (2008-2013). Microchim. Acta *181*, 865–891.

42. Taufiq, S., Waqar, M., Sharif, M.N., and Abbas, S.R. (2023). Towards portable rapid TB biosensor: Detecting Mycobacterium tuberculosis in raw sputum samples using functionalized screen printed electrodes. Bioelectrochemistry *150*, 108353. https://doi.org/10.1016/J.BIOELECHEM.2022.108353.

43. Bonaldo, S., Cretaio, E., Pasqualotto, E., Scaramuzza, M., Franchin, L., Poggi, S., and Paccagnella, A. (2023). Screen-Printed Electrochemical Biosensor for the Detection of Bacteriophage of Lactococcus Lactis for Dairy Production. IEEE Sens. J. *23*, 5552–5560. https://doi.org/10.1109/JSEN.2023.3242107.

44. Hu, Y., Zhang, Z., Mei, A., Jiang, Y., Hou, X., Wang, Q., Du, K., Rong, Y., Zhou, Y., Xu, G., and Han, H. (2018). Improved Performance of Printable Perovskite Solar Cells with Bifunctional Conjugated Organic Molecule. Adv. Mater. *30*, 1705786. https://doi.org/10.1002/ADMA.201705786.

45. Ryu, J., Lee, K., Yun, J., Yu, H., Lee, J., and Jang, J. (2017). Paintable Carbon-Based Perovskite Solar Cells with Engineered Perovskite/Carbon Interface Using Carbon Nanotubes Dripping Method. Small *13*, 1701225. https://doi.org/10.1002/SMLL.201701225.

46. Hyun, W.J., Secor, E.B., Hersam, M.C., Frisbie, C.D., and Francis, L.F. (2015). High-Resolution Patterning of Graphene by Screen Printing with a Silicon Stencil for Highly Flexible Printed Electronics. Adv. Mater. *27*, 109–115. https://doi.org/10.1002/ADMA.201404133.
47. Liang, J., Tong, K., and Pei, Q. (2016). A Water-Based Silver-Nanowire Screen-Print Ink for the Fabrication of Stretchable Conductors and Wearable Thin-Film Transistors. Adv. Mater. *28*, 5986–5996. https://doi.org/10.1002/ADMA.201600772.
48. Ren, H., Zhang, X., Liu, Q., Tang, W., Liang, J., and Wu, W. (2024). Fully-Printed Flexible Aqueous Rechargeable Sodium-Ion Batteries. Small *20*, 2312207. https://doi.org/10.1002/SMLL.202312207.
49. Molaiyan, P., Valikangas, J., Sliz, R., Ramteke, D.D., Hu, T., Paolella, A., Fabritius, T., and Lassi, U. (2024). Screen-Printed Composite LiFePO4-LLZO Cathodes Towards Solid-State Li-ion Batteries. Chemelectrochem *11*, e202400051. https://doi.org/10.1002/CELC.202400051.
50. Kim, T.Y., Im, C.Y., Choi, J.H., Gu, D., Yoon, S., Kim, U.-H., Kim, S.J., Kim, T.Y., Im, C.Y., Choi, J.H., et al. (2024). Fabrication of a Porous Copper/Graphite/Zirconium Oxide Hybrid Anode via Screen Printing for Lithium-Ion Batteries. Adv. Funct. Mater. *34*, 2411648. https://doi.org/10.1002/ADFM.202411648.
51. Gören, A., Mendes, J., Rodrigues, H.M., Sousa, R.E., Oliveira, J., Hilliou, L., Costa, C.M., Silva, M.M., and Lanceros-Méndez, S. (2016). High performance screen-printed electrodes prepared by a green solvent approach for lithium-ion batteries. J. Power Sources *334*, 65–77. https://doi.org/10.1016/J.JPOWSOUR.2016.10.019.
52. Liu, J., Jiang, X., Zhang, R., Zhang, Y., Wu, L., Lu, W., Li, J., Li, Y., and Zhang, H. (2019). MXene-Enabled Electrochemical Microfluidic Biosensor: Applications toward Multicomponent Continuous Monitoring in Whole Blood. Adv. Funct. Mater. *29*, 1807326. https://doi.org/10.1002/ADFM.201807326.
53. Jin, X., Li, G., Xu, T., Su, L., Yan, D., and Zhang, X. (2022). Fully integrated flexible biosensor for wearable continuous glucose monitoring. Biosens. Bioelectron. *196*, 113760. https://doi.org/10.1016/J.BIOS.2021.113760.
54. Krebs, F.C. (2009). Fabrication and processing of polymer solar cells: A review of printing and coating techniques. Sol. Energy Mater. Sol. Cell. *93*, 394–412. https://doi.org/10.1016/J.SOLMAT.2008.10.004.
55. Yu, L., Fan, Z., Shao, Y., Tian, Z., Sun, J., and Liu, Z. (2019). Versatile N-Doped MXene Ink for Printed Electrochemical Energy Storage Application. Adv. Energy Mater. *9*, 1901839. https://doi.org/10.1002/AENM.201901839.
56. Abdolhosseinzadeh, S., Schneider, R., Verma, A., Heier, J., Nüesch, F., and Zhang, C.J. (2020). Turning Trash into Treasure: Additive Free MXene Sediment Inks for Screen-Printed Micro-Supercapacitors. Adv. Mater. *32*, 2000716. https://doi.org/10.1002/ADMA.202000716.
57. Zavanelli, N., and Yeo, W.-H. (2021). Advances in Screen Printing of Conductive Nanomaterials for Stretchable Electronics. ACS Omega *6*, 9344–9351. https://doi.org/10.1021/acsomega.1c00638.
58. Bai, Y., Wang, H., Xue, Y., Pan, Y., Kim, J.T., Ni, X., Liu, T.L., Yang, Y., Han, M., Huang, Y., et al. (2022). A dynamically reprogrammable surface with self-evolving shape morphing. Nature *609*, 701–708. https://doi.org/10.1038/s41586-022-05061-w.
59. Zou, S., Picella, S., de Vries, J., Kortman, V.G., Sakes, A., and Overvelde, J.T.B. (2024). A retrofit sensing strategy for soft fluidic robots. Nat. Commun. *15*, 539. https://doi.org/10.1038/s41467-023-44517-z.
60. Shintake, J., Cacucciolo, V., Floreano, D., and Shea, H. (2018). Soft Robotic Grippers. Adv. Mater. *30*, 1707035. https://doi.org/10.1002/ADMA.201707035.
61. Qi, Z., Zhou, M., Li, Y., Xia, Z., Huo, W., Huang, X., Qi, Z., Zhou, M., Li, Y., Xia, Z., et al. (2021). Reconfigurable Flexible Electronics Driven by Origami Magnetic Membranes. Adv. Mater. Technol. *6*, 2001124. https://doi.org/10.1002/ADMT.202001124.
62. Kim, Y., Yuk, H., Zhao, R., Chester, S.A., and Zhao, X. (2018). Printing ferromagnetic domains for untethered fast-transforming soft materials. Nature *558*, 274–279. https://doi.org/10.1038/S41586-018-0185-0.
63. Zhou, L., Ren, L., Chen, Y., Niu, S., Han, Z., and Ren, L. (2021). Bio-Inspired Soft Grippers Based on Impactive Gripping. Adv. Sci. *8*, 2002017. https://doi.org/10.1002/ADVS.202002017.
64. Andika, I.B., Wei, S., Cao, C., Salaipeth, L., Kondo, H., and Sun, L. (2017). Phytopathogenic fungus hosts a plant virus: A naturally occurring cross-kingdom viral infection. Proc. Natl. Acad. Sci. USA *114*, 12267–12272.
65. Jeng, M.-L., and Jeng, M.-L. (2019). Biofluorescence in Terrestrial Animals, with Emphasis on Fireflies: A Review and Field Observation. In Bioluminescence - Analytical Applications and Basic Biology. https://doi.org/10.5772/INTECHOPEN.86029.
66. Wang, Z., Misra, S., and Venkiteswaran, V.K. (2024). Fluidic control programming for 3D magnetic soft metamaterials with reconfigurable mechanical behaviors. Cell Rep. Phys. Sci. *5*, 102125. https://doi.org/10.1016/j.xcrp.2024.102125.